

Intermolecular Proton Transfer in Microhydrated Guanine–Cytosine Base Pairs: a New Mechanism for Spontaneous Mutation in DNA

J. P. Cerón-Carrasco,* A. Requena, and J. Zúñiga

Departamento de Química Física, Facultad de Química, Universidad de Murcia, Campus de Espinardo, 30100 Murcia, Spain

C. Michaux†

Laboratoire de Chimie Biologique Structurale, Facultés Universitaires Notre-Dame de la Paix, Rue de Bruxelles, 61, 5000 Namur, Belgium

E. A. Perpète‡ and D. Jacquemin§

Laboratoire de Chimie Théorique Appliquée, Facultés Universitaires Notre-Dame de la Paix, Rue de Bruxelles, 61, 5000 Namur, Belgium

Received: July 11, 2009; Revised Manuscript Received: August 3, 2009

Accurate calculations of the double proton transfer (DPT) in the adenine–thymine base pair (AT) were presented in a previous work [*J. Phys. Chem. A* 2009, 113, 7892.] where we demonstrated that the mechanism of the reaction in solution is strongly affected by surrounding water. Here we extend our methodology to the guanine–cytosine base pair (GC), for which it turns out that the proton transfer in the gas phase is a synchronous concerted mechanism. The O(G)–H–N(C) hydrogen bond strength emerges as the key parameter in this process, to the extent that complete transfer takes place by means of this hydrogen bond. Since the main effect of the molecular environment is precisely to weaken this bond, the direct proton transfer is not possible in solution, and thus the tautomeric equilibrium must be assisted by surrounding water molecules in an asynchronous concerted mechanism. This result demonstrates that water plays a crucial role in proton reactions. It does not act as a passive element but actually catalyzes the DPT.

I. Introduction

Since Watson and Crick published their seminal article in 1953,¹ the interactions between the hydrogen bonds in DNA base pairs have attracted a broad interest from both experimental and theoretical chemists. Given their double helix structure, the interactions between base pairs are responsible for the storage and transfer of the genetic information. Consequently, genomic sequence alterations through different mechanisms like formation of wobble base pairs, geometric discrimination or electrostatic preorganization of the deoxyribonucleotide triphosphates (dNTPs) substrates could increase the possibility of spontaneous mutations during DNA replication.^{2–4} Besides, on the basis of the Watson–Crick’s model, Löwdin introduced the hypothesis that “rare” tautomers could be formed via the double proton transfer (DPT) mechanism,^{5,6} and suggested that spontaneous mutagenesis could be also induced by these variations of the tautomeric state of the nucleotide bases.

Following Löwdin’s work, the DNA base pairs have been extensively studied using a wide range theoretical approaches, essentially in the gas phase.^{7–23} However, under physiological conditions, water molecules are critical to ensure DNA’s stability,^{24,25} and the aqueous environment also affects the structure and functionality of nucleic acids.²⁶ To provide a more realistic model for DNA, several theoretical studies have been

carried out to establish the influence of hydration on the tautomeric equilibrium and related properties.^{26–43} The first study that addressed this topic was conducted by Florián and co-workers,²⁷ who found that polar environments stabilize the canonical structure with respect to “rare” tautomers. This result is consistent with the recent work by Gorb and co-workers²⁶ and supports the importance of water molecules in tautomeric equilibrium. Furthermore, the chemical environment effects have been considered by Kumar and co-workers,^{42,43} who built up so-called solution models for microhydrated adenine–thymine (AT) and guanine–cytosine (GC) pairs. On the other hand, Lee and Cho³⁷ focused on the influence of solvent molecules on the vibrational properties of such base pairs. Specifically, these authors observed a frequency shift of the modes related to the H-bonding interactions between base pairs and surrounding water molecules. This findings are consistent with the results published by Herbert and co-workers,³⁸ who evaluated solvation effects on interbase bond strengths. Regarding tautomeric equilibrium, Kabelác and Hobza³⁹ have recently shown that surrounding water molecules may tune the relative stability of the base pairs. To the best of our knowledge, only a few papers have considered intramolecular proton transfer assisted by water molecules in a single base,^{44–47} and we have recently studied, in a previous work, the mechanism of the catalytic role of water for DPT in the adenine–thymine base pair.⁴⁸

Of course, there are essential differences between AT and GC pairs. First, the interaction energy in GC has been estimated to be approximately twice that of AT.^{49–51} the hydrogen bonds between guanine and cytosine are stronger than between adenine and

* Corresponding author. E-mail: jpceron@um.es.

† Scientific Research Worker of the Belgian FNRS.

‡ Senior Research Associate of the Belgian FNRS. E-mail: eperpette@fundp.ac.be.

§ Research Associate of the Belgian FNRS.

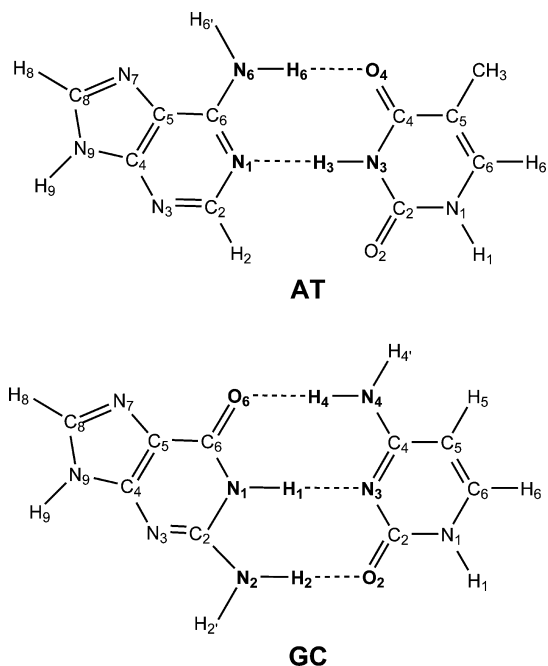


Figure 1. Watson–Crick adenine–thymine (AT) and guanine–cytosine (GC) base pair structures.

thymine. Moreover, in the case of GC we have three hydrogen bonds (Figure 1), making it possible proton transfer mechanisms to be more abundant and complex. Previous studies have predicted that in the gas phase AT does not allow the formation of “rare” tautomers,^{7,18} though it has been suggested^{8,19,26,27} that an efficient DPT mechanisms may exist in GC to promote the product usually labeled as GC2 (Figure 2). It is worth noting that Florian and Leszczynski⁸ studied two additional tautomeric forms: GC3 and GC4 (Figure 3). The former corresponds to another direct proton transfer product, whereas the latter is reached through the migration of the proton H4' (not included in interbase hydrogen bonds) from cytosine to guanine, by a flip-flop mechanism.⁵²

According to our previous study on AT,⁴⁸ proton transfer mechanisms can be affected by the chemical environment, and consequently surrounding water molecules may play an important role in spontaneous mutation in DNA. In this paper, we extend this study to the GC base pair. We have designed several first hydration shell models to investigate the impact of water on the geometries of the GC complex, as well as its catalytic role during the proton transfer between these two bases. Comparisons between DPT mechanisms in the gas phase and in solution are also presented.

II. Computational Methods

All the structures have been fully optimized using the BP86^{53,54} functional in connection with Pople's 6-311++G(d,p) basis set, and free of any symmetry restriction, i.e., in the C_1 symmetry group. We have chosen this theoretical level because it was shown to be able to provide the best accuracy/computational cost ratio for AT in both the gas and condensed phase.⁴⁸ Moreover, we have compared our BP86 results with the experimental and theoretical data available in the literature for GC^{8,19,26,50,51,55} (see the next section). The influence of the basis set superposition error (BSSE) in the final geometries and relative energies was also assessed within the counterpoise (CP) scheme⁵⁶ by computing the geometries in two different ways: (i) the geometries obtained without BSSE corrections are used for single point energy calculations; (ii) full BSSE corrections

are performed during the force minimization process,⁵⁷ as we recently demonstrated the importance of such corrections in water–amino acids complexes.^{58,59} The harmonic vibrational frequencies and thermodynamic corrections at 298 K were obtained at a consistent theoretical level. The vibrational analysis confirms the nature of the stationary points: free imaginary frequency for a minimum, and one single imaginary value for a transition state (TS). The corresponding total energies of all the stationary points have been improved using the MP2/infinite basis set extrapolation developed by Truhlar,⁶⁰ which provides the most accurate results according to a recent benchmark study of the gas phase GC.⁵⁰ The basis set extrapolation is based on a split of the total energy into its Hartree–Fock and correlation parts:

$$E^{\text{tot}} = E^{\text{HF}} + E^{\text{cor}} \quad (1)$$

According to Truhlar's method, the basis-set limit for the total energy is calculated by the following equation:

$$E_{\infty}^{\text{tot}} = \frac{3^{\alpha}}{3^{\alpha} - 2^{\alpha}} E_X^{\text{HF}} - \frac{2^{\alpha}}{3^{\alpha} - 2^{\alpha}} E_Y^{\text{HF}} + \frac{3^{\beta}}{3^{\beta} - 2^{\beta}} E_X^{\text{cor}} - \frac{2^{\beta}}{3^{\beta} - 2^{\beta}} E_Y^{\text{cor}} \quad (2)$$

where Y and X denote the cc-pVDZ and the cc-pVTZ basis sets, respectively, while α and β are fitting exponents. For the particular case of MP2 method, these exponents are $\alpha = 3.4$ and $\beta = 2.2$. We obtain the Gibbs free energies ΔG^0 from the total electronic energies and the thermal corrections, and the equilibrium constant is calculated using:

$$K_{\text{eq}} = e^{-\Delta G^0/RT} \quad (3)$$

All our calculations were carried out with the Gaussian 03 package,⁶¹ while the normal vibration mode visualizations were performed using the Molekel program.⁶²

III. Results and Discussion

A. GC in the Gas Phase. First, we check the ability of the selected theoretical scheme to accurately describe both the geometry and the complexation energy of GC in the gas phase. Table 1 shows the major geometric parameters involved in the three hydrogen bonds, together with previous results available in the literature⁵⁵ as well as the benchmark MP2 values.⁵⁰ According to the mean absolute deviation (MAD) calculated for the hydrogen bond distances, BP86/6-311++G(d,p) is indeed suitable, as it meets the reference data at much smaller computational costs. Furthermore, we can neglect the BSSE effects during the geometry optimizations as the CP corrections modify the bond distances by less than 0.02 Å. As the DFT complexation energies for all functionals spread over a 3–5 kcal/mol range, the BSSE effects are negligible. On the other hand, single point calculations at the MP2/infinite level using the BP86/6-311++G(d,p) geometry yield energies in very good agreement with RI-MP2 and CCSD(T) values, especially when BSSE corrections are taken into account. Here, only the relative energies for different tautomeric forms of GC are of interest; i.e., the values of absolute energies are meaningless. As a result, we can state that MP2/infinite//BP86/6-311++G(d,p), is sufficiently accurate for our study.

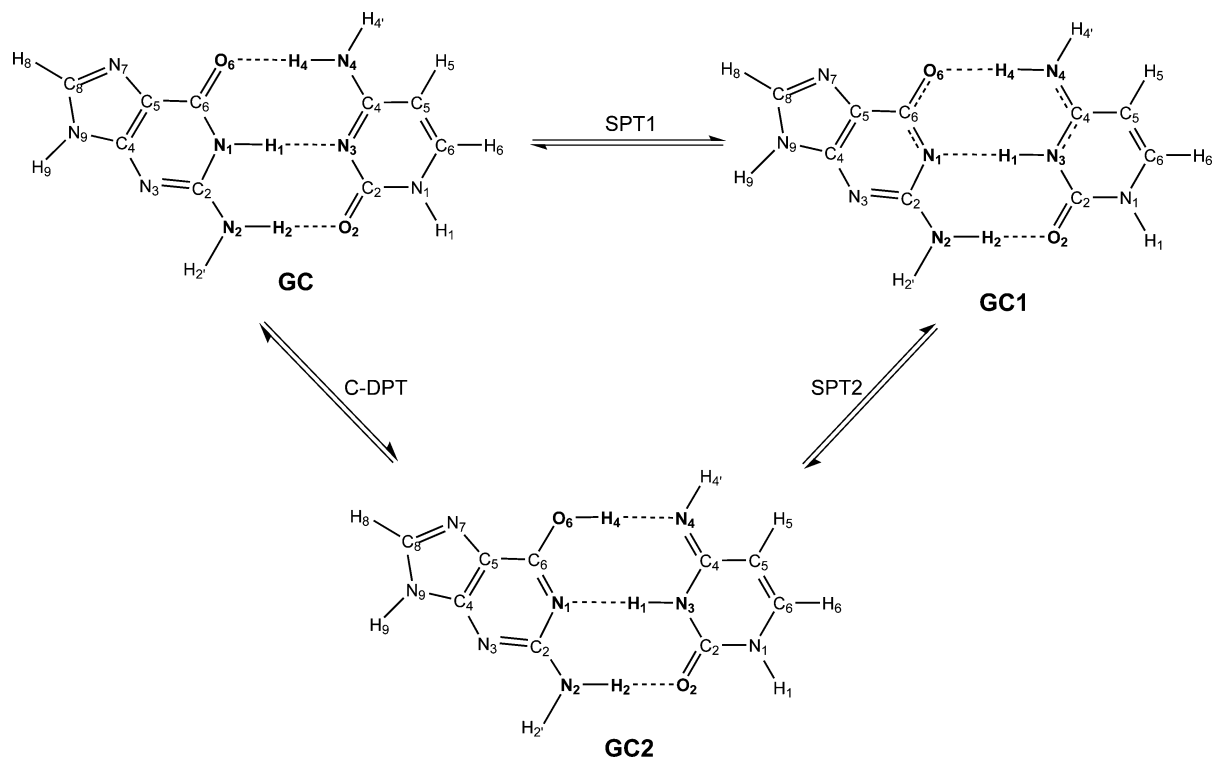


Figure 2. Double proton transfer (DPT) in GC base pair. This reaction may take place through a concerted (C-DPT) or via a stepwise mechanism following two different single proton transfer steps (SPT1 and SPT2).

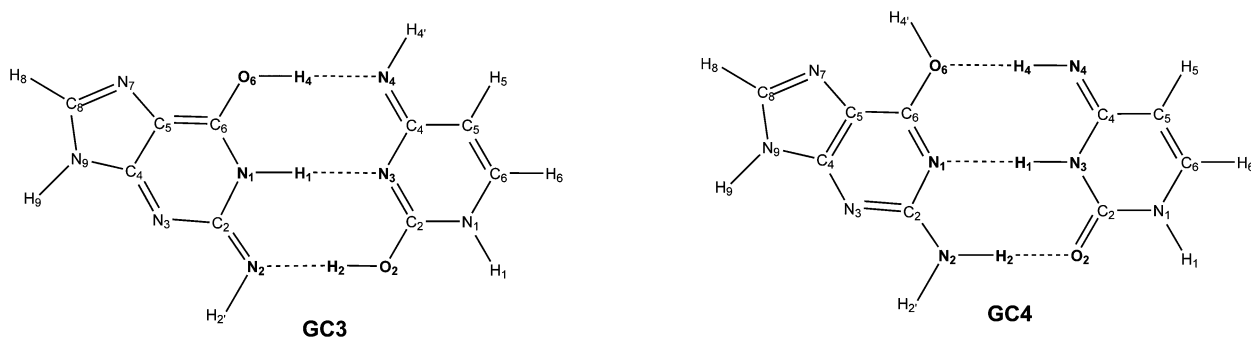


Figure 3. Chemical structure for GC3 and GC4 tautomers.

TABLE 1: Interbase Hydrogen-Bond Distances (Å) and Complexation Energies (kcal/mol) Calculated for GC in Gas the Phase within Several Theoretical Schemes

method	geometry				energy		
	O6–N4	N1–N3	N2–O2	MAD ^a	ΔE	BSSE	ΔE_{BSSE}^b
Benchmark Values							
RI-MP2/aug-cc-pVQZ//RI-MP2/cc-pVTZ ^c	2.75	2.90	2.89				–27.7
CCSD(T)/aug-cc-pVQZ//RI-MP2/cc-pVTZ ^d	2.75	2.90	2.89				–28.2
DFT Calculations							
B3LYP/cc-pVTZ ^e	2.79	2.94	2.93	0.040	–26.1	1.7	–24.4
BLYP/cc-pVTZ ^e	2.80	2.96	2.96	0.060	–24.6	2.0	–22.6
BP86/cc-pVTZ ^e	2.73	2.90	2.89	0.007	–26.6	1.8	–24.8
BP86/6-311++G(d,p)	2.75	2.91	2.90	0.007	–26.0	1.1	–24.9
BP86/6-311++G(d,p) ^f	2.77	2.92	2.92	0.023		1.1	–25.0
Basis Set Extrapolation							
MP2/infinite//BP86/6-311++G(d,p)	2.75	2.91	2.90	0.007	–29.1	1.9	–27.2

^a MAD: mean absolute deviation of the theoretical distances with respect to the benchmark values. ^b Bond energy with BSSE corrections. ^c From ref 50. ^d From ref 51. ^e From ref 55. ^f BSSE included during the geometry optimization process.

Taking into account these preliminary results, we proceed to the study of the DPT reaction between the guanine and cytosine base pair in the gas phase. According to our calculations, there are three minima in the gas phase: GC, GC2, and GC4 (Figures

2 and 3). The canonical form (GC) is the most stable structure, whereas the tautomers GC2 and GC4 are 7.80 and 15.6 kcal/mol above the global minimum, respectively. Consequently, the formation of GC4 is unlikely, and we take only GC2 into

TABLE 2: Theoretical Bond Distances and Interbase Hydrogen Bonds (Å) Calculated for GC Double Proton Transfer Mechanism in the Gas Phase (see Figure 2)

method	BSSE ^a	N2–H2	O2–H2	N1–H1	N3–H1	O6–H4	N4–H4
GC							
BP86/6-311++G(d,p)		1.034	1.872	1.049	1.859	1.699	1.055
BP86/6-311++G(d,p)	✓	1.033	1.887	1.048	1.872	1.709	1.054
B3LYP/cc-pVDZ ^b		1.027	1.890	1.039	1.877	1.723	1.045
B3LYP/cc-pVDZ ^b	✓	1.025	1.929	1.037	1.911	1.755	1.041
B3LYP/6-31G(d) ^c		1.02	1.91	1.03	1.92	1.78	1.04
MP2/6-31G(d) ^c		1.02	1.94	1.04	1.93	1.82	1.03
HF/6-31G(d) ^d		1.002	2.016	1.008	2.036	1.922	1.009
GC2 [‡]							
BP86/6-311++G(d,p)		1.031	1.835	1.388	1.247	1.157	1.342
B3LYP/6-31G(d) ^c		1.02	1.83	1.32	1.29	1.12	1.38
MP2/6-31G(d) ^c		1.02	2.02	1.54	1.14	1.38	1.15
HF/6-31G(d) ^d		0.999	1.872	1.326	1.283	1.160	1.282
GC2							
BP86/6-311++G(d,p)		1.026	1.939	1.756	1.077	1.039	1.613
BP86/6-311++G(d,p)	✓	1.025	1.952	1.776	1.074	1.036	1.628
B3LYP/cc-pVDZ ^b		1.020	1.961	1.808	1.057	1.013	1.687
B3LYP/cc-pVDZ ^b	✓	1.019	2.007	1.855	1.052	1.010	1.724
B3LYP/6-31G(d) ^c		1.02	1.99	1.87	1.05	1.01	1.74
MP2/6-31G(d) ^c		1.02	2.02	1.89	1.04	1.01	1.78
HF/6-31G(d) ^d		0.997	2.138	2.046	1.012	0.967	1.912

^a BSSE included during the geometry optimization process. ^b From ref 19. ^c From ref 26. ^d From ref 8.

account. In Table 2 we compare the optimized geometries for GC and GC2 with results available in the literature. The optimized geometry of the transition state labeled as GC2[‡], which connects GC to GC2, is also shown in Table 2, as this geometry provides a relevant information about the mechanism of the reaction. We can deduce from the BP86/6-311++G(d,p) bond distances that the proton transfer in GC is a concerted and synchronous mechanism. This result agrees with the analysis of the vibrational imaginary frequency mode at 970i cm⁻¹, associated to the simultaneous N1–H1 and H4–N4 stretching (see details in the Supporting Information).

From the data in Table 2, it is obvious that B3LYP overestimates the hydrogen bond distances even in combination with the cc-pVDZ basis set, consistently with the ref 55. Furthermore, the bond distances calculated with MP2/6-31G(d) or HF/6-31G(d) also appear to be overestimated. This demonstrates, on the one hand, that the inclusion of correlation effects is definitely required for the study of GC and, on the other hand, that 6-31(d) is not flexible enough to describe hydrogen bonds: more extended basis sets are mandatory. It is worth mentioning that the Gorb and co-workers' MP2/6-31G(d) study foresees an asynchronous transfer, while B3LYP/6-31G(d) yields to a synchronous mechanism, as we can deduce by analyzing the geometries of TS listed in Table 2. Since our BP86/6-311++G(d,p) provides the closest results to the benchmark geometry, we state that the pathway for DPT between GC in the gas phase must be closer to synchronous mechanism, contrary to the MP2/6-31G(d) prediction. Finally, we do not observe any significant difference in bond distance when BSSE corrections are included in the optimization process, confirming that this effect is insignificant for the structural data.

To get more valuable insights, we have also calculated the relative Gibbs free energies at 298 K, which are given in Table 3. Unlike the results obtained for the proton transfer in AT,⁴⁸ where only the canonical form was found stable in the gas phase, the proton transfer in GC is a thermodynamical possible reaction, with an equilibrium constant in the range of 10⁻⁷. To understand this difference, let us think in terms of an asynchronous mechanism in which DPT is decomposed into two steps:

TABLE 3: Total Electronic Energy (*E*/au), Relative Energy (ΔE /kcal mol⁻¹), and Relative Gibbs Free Energies at 298 K (ΔG /kcal mol⁻¹) Calculated for DPT Reaction in the Gas Phase

structure	E_{∞}^{tot}	ΔE	ΔG^0	K_{eq}
GC	-936.37323	0.00	0.00	
GC2 [‡]	-936.35339	12.45	9.72	
GC2	-936.36081	7.80	8.28	8.4×10^{-7}

initially, the first proton is transferred (H3 in AT, and H1 in GC) achieving the zwitterionic intermediate (AT1 or GC1), and in the second step, the migration of the second proton leads to the final DPT product. There is, of course, an alternative path that allows for the electrical neutrality to be recovered: the proton moving in the first step can return to its original position leading to canonical form. What are then the conditions favoring the second DPT step? To answer this question, let us compare the strengths of the hydrogen bonds not involved in the first proton transfer by analyzing the geometrical parameters. According to our previous study,⁴⁸ the optimized H6–O4 bond distance for canonical AT pair (Figure 1) is 1.854 Å, whereas for GC we see in Table 2 that the optimized O2–H2, and O6–H4 bond distances (Figure 1) are 1.872 and 1.699 Å, respectively. These data indicate then that the strong O6–H4 hydrogen bond in GC, nonexistent in AT, promotes the second proton transfer. Note that the relative Gibbs free energies listed in Table 3 totally support the above hypothesis. Also, from a methodological point of view, the fact that DFT calculations provide a shorter O6–H4 bond than MP2/6-31G(d) may explain why DFT foresees a synchronous mechanism, whereas MP2 suggests an asynchronous transfer.

B. Model for DPT in Solvated GC. Although BP86/6-311++G(d,p) hydrogen bond lengths are in very good agreement with the “best” benchmark values in the gas phase, significant discrepancies between theoretical geometries and experimental data⁶³ can be found. As noted by Guerra and co-workers,⁶⁴ this disagreement is due to a deficiency of the gas phase model. By incorporating the effects of the molecular environment to the AT and GC models, they obtained geometries closer to the experiment.⁵⁵ Accordingly, we also extended

our gas phase methodology by including surrounding molecules to simulate a more realistic biological environment.

We consider environment effects on the structure of GC models recently published by Wijst and co-workers (GC-a and GC-b),⁵⁵ and by Kumar et al. (GC-e and GC-d).⁴³ Furthermore, a new model (GC-c) was built up in which we have included only the four water molecules complexed to the atoms involved in the intramolecular hydrogen bonds. Then, we check how these models approach the experimental hydrogen bond distances. In the particular case of Wijst and co-workers' GC-a model, the optimized geometry presents one imaginary frequency around $300i\text{ cm}^{-1}$, which can be mainly interpreted as the rotation of the water molecule complexed to proton H2' of guanine. Consequently, we modify the geometry of the GC-a model to achieve a real minimum. All optimized chemical structures of all solvated models are displayed in Figure 4.

The hydrogen bond lengths for each model are listed in Table 4, and it can be seen that the hydrogen bonds are weaker in solution than in the gas phase, as illustrated by the longer distances in the former case. However, while the N1–N3 and N2–O2 distance remains almost constant, a significant modification is observed for O6–N4, with calculated bond lengths in the range 2.80–2.94 Å, closer to the experiment value of 2.93 Å. Indeed, these distances in both GC-a and GC-b are in very good agreement with X-ray structure. For the models solely including water molecules, i.e., no counterion (GC-c, GC-d and GC-e), we obtain a gradual improvement when the number of water molecules is increased. According to our calculations, the geometries obtained with the two selected basis sets are practically the same, and 6-311++G(d,p) can be considered adequate and sufficient for the theoretical study of such system.

It is important to emphasize that the main effect of the chemical environment is precisely to weaken the key O6–N4 bond, surprisingly the strongest in the gas phase. Therefore, to check our hypothesis regarding the importance of this bond in the DPT process, we optimized the geometries of all "rare" tautomers for the five proposed solvated models. The canonical base pair is, like in the gas phase, the most stable structure whatever the model, and no other stable tautomer could be found for GC1, GC2, or GC3, despite several tries. This backs up our stability hypothesis and also explains why surrounding water molecules can displace the tautomeric equilibrium toward the canonical form.

On the other hand, GC4 can now be considered as the product of an assisted proton transfer, and consequently for solvated models GC-c, GC-d, and GC-e (where water molecules allow an efficient catalysis), GC4 structures can be identified. In this case, water molecules act directly as proton donor and proton acceptor, and subsequently catalyze the DPT process. Figure 5 summarizes the results for this alternative mechanism in solution. An analysis of the TS geometries and vibrational modes allows the mechanism of the proton transfer to be pinpointed. It turns out that the H1–N3 bond distance in the TS geometry is similar to the equilibrium geometry for the catalyzed DPT products. In addition, we obtain only one imaginary frequency, which can be interpreted as the simultaneous stretching of the N4–H4' bond and of all the water bonds involved in the catalyzed proton transfer. This imaginary frequency is $1058i$, $851i$, and $886i\text{ cm}^{-1}$ for GC4[‡]-c, GC4[‡]-d, and GC4[‡]-e, respectively (vibrational modes analysis is detailed in the Supporting Information). The catalyzed DPT process in solution therefore corresponds to an asynchronous concerted mechanism, in which in the first step the proton H1 migrates from N1 to N3 (see

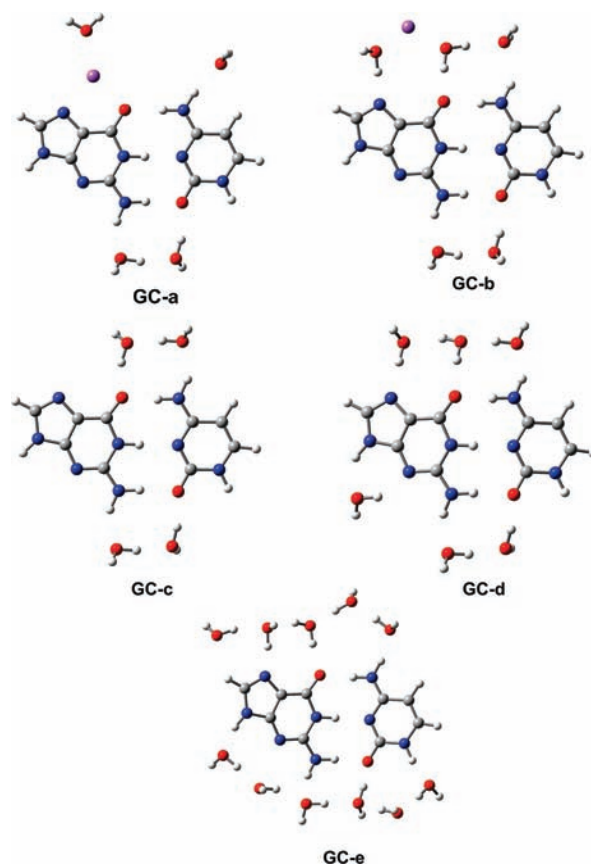


Figure 4. Optimized geometries for solution models (see text). Carbon atoms are in gray, nitrogen in blue, hydrogen in white, and sodium in purple.

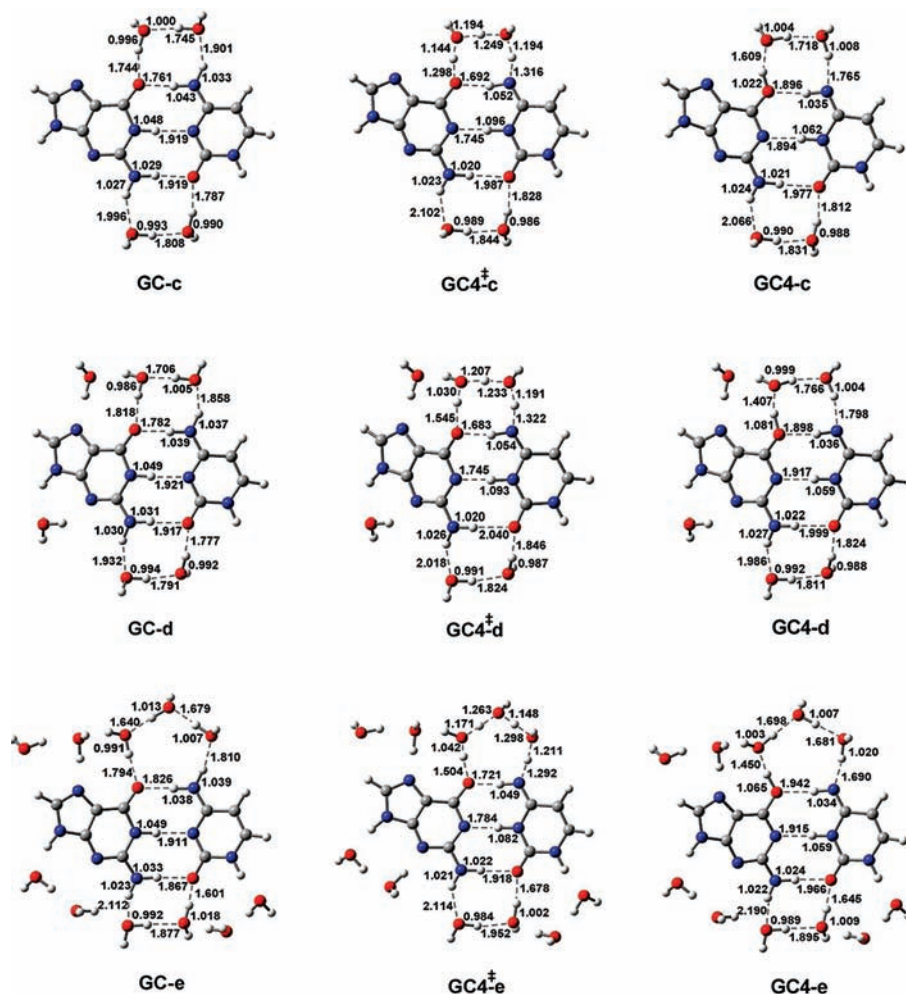
Figure 1) and is followed by an assisted proton transfer, leading to the final DPT product, which is GC4.

Finally, let us discuss the thermodynamical data presented in Table 5. From the relative Gibbs energies, it can be concluded that the tautomeric equilibrium is significantly affected by the number of water molecules in the solution model. Increasing the number of water molecules from 4 to 6 decreases the activation barriers and stabilizes the final product. Including 11 water molecules yields an extra decrease of the activation barrier, but only a negligible variation of the relative energy of the product. The resulting energies suggest that (i) 6 water molecules are enough to achieve the limit of GC4 stabilization and (ii) the proton transfer assisted by three water molecules is more probable than the two-water-aided process. It has already been mentioned that proton transfers are subject to the tunneling effect and thermal fluctuations,⁶⁵ and, for this reason, the activation barriers of Table 5 are only indicative. We have also estimated the magnitude of the equilibrium constant for the catalyzed mechanism. From the comparison of data shown in Table 3 with the GC-d and GC-e relative Gibbs energies (models that provide the accurate hydrogen bonds and allow water-catalyzed DPT), it can be concluded that the equilibrium constant in solution is 4 orders of magnitude smaller than in the gas phase. We should note that despite the stability of the tautomeric forms is found to be very low when solvated models are used, the prediction of the equilibrium constants for the GC-d and GC-e models are in satisfactory agreement with the frequency of observable natural spontaneous mutations, which is also very low (between 10^{-8} and 10^{-10}).⁶⁶

TABLE 4: Interbase Hydrogen-Bond Lengths (Å) for Several GC Models in Solution

bond	exp ^a	BP86/cc-pVTZ		BP86/6-311++G(d,p)				
		GC-a ^b	GC-b ^c	GC-a	GC-b	GC-c	GC-d	GC-e
O6–N4	2.91	2.94	2.87	2.94	2.87	2.80	2.81	2.85
N1–N3	2.95	2.93	2.97	2.93	2.96	2.97	2.95	2.94
N2–O2	2.86	2.86	2.89	2.87	2.90	2.95	2.94	2.88
MAD ^c		0.017	0.030	0.020	0.030	0.073	0.060	0.030

^a X-ray crystallographic measurements from ref 63. ^b Geometry with all frequencies real. ^c From ref 55. ^c Mean absolute deviation for theoretical distances.

**Figure 5.** Optimized structures for DPT reaction in the solution model. The bond distances for the main geometrical parameters are given in Å.

IV. Conclusions

The double proton transfer in the guanine–cytosine base pair has been studied theoretically using ab initio calculations in the gas phase and with five solvated models. By analyzing the optimized geometries, vibrational frequencies and relative energies, we have deduced that the MP2/infinite//BP86/6-311G(d,p) approach provides accurate results at a fairly reasonable computational price. Using this theoretical level, we demonstrate that the DPT is a thermodynamic possible process in the gas phase due to the strength of O6–H4 hydrogen bond: the GC2 tautomer is the most likely product. Furthermore, the analysis of TS suggests that the proton transfer is a synchronous concerted mechanism. The main effect of molecular environment is the weakening of the O6–N4 hydrogen bond, and consequently the direct proton transfer is not possible in solution. Our calculations show,

TABLE 5: Total Electronic Energy (E/au), Relative Energy ($\Delta E/\text{kcal mol}^{-1}$), and Relative Gibbs Free Energies at 298 K ($\Delta G^0/\text{kcal mol}^{-1}$) Calculated for DPT Reaction in Solution Models

Structure	$E_{\text{tot}}^{\text{tot}}$	ΔE	ΔG^0	K_{eq}
Model GC-c				
GC-c	-1241.92190	0.00	0.00	
GC4 [‡] -c	-1241.87454	29.72	26.69	
GC4-c	-1241.89668	15.83	16.68	5.9×10^{-13}
Model GC-d				
GC-d	-1394.70443	0.00	0.00	
GC4 [‡] -d	-1394.66607	24.08	21.08	
GC4-d	-1394.68033	15.13	14.22	7.3×10^{-11}
Model GC-e				
GC-e	-1776.64201	0.00	0.00	
GC4 [‡] -e	-1776.60787	21.43	17.36	
GC4-e	-1776.61739	15.45	14.29	3.3×10^{-11}

however, that the water-assisted transfer provides a thermodynamically accessible path for DPT in solution. According to the TS, the reaction follows in this case an asynchronous concerted mechanism.

These solution models are of course a first approximation to the real environment of the solvated DNA, but the results reported in this paper clearly help to understand the DPT mechanisms between DNA base pairs in solution and emphasize the role that water molecules may play.

Acknowledgment. We thank Professor A. Kumar at Oakland University for supplying the initial geometries of GC-d and GC-e models. The work was partially supported by the Ministerio de Ciencia e Innovación of Spain under Project CTQ2007-66528, and by the Fundación Séneca del Centro de Coordinación de la Investigación de la Región de Murcia under Project 08735/PI/08. J.P.C.C. acknowledges a fellowship provided by the Ministerio de Ciencia e Innovación of Spain. E.A.P., C.M., and D.J. thank the Belgian National Fund for their respective positions. Most calculations have been performed on the Interuniversity Scientific Computing Facility (ISCF), installed at the Facultés Universitaires Notre-Dame de la Paix (Namur, Belgium), for which the authors gratefully acknowledge the financial support of the FNRS-FRFC and the “Loterie Nationale” for convention number 2.4578.02 and of the FUNDP.

Supporting Information Available: (1) Cartesian coordinates of all optimized transition states geometries at the BP86/6-311++G(d,p) level. (2) Visualization (mpg files) of the normal modes with the imaginary frequency for transitions states. This material is available free of charge via the Internet at <http://pubs.acs.org>.

References and Notes

- Watson, J.; Crick, F. *Nature* **1953**, *171*, 737–738.
- Florián, J.; Goodman, M.; Warshel, A. *J. Phys. Chem. B* **2002**, *106*, 5739–5753.
- Florián, J.; Goodman, M.; Warshel, A. *J. Phys. Chem. B* **2002**, *106*, 5754–5760.
- Florián, J.; Goodman, M.; Warshel, A. *Proc. Natl. Acad. Sci. U.S.A.* **2005**, *102*, 6819–6824.
- Löwdin, P. *Rev. Mod. Phys.* **1963**, *35*, 724–732.
- Löwdin, P. *Electronic Aspects of Biochemistry*; Academic Press: New York, 1964.
- Florián, J.; Hroudá, V.; Hobza, P. *J. Am. Chem. Soc.* **1994**, *116*, 1457–1460.
- Florián, J.; Leszczynski, J. *J. Am. Chem. Soc.* **1996**, *118*, 3010–3017.
- Marañón, J.; Fontani, A.; Grigera, J. *J. Theor. Biol.* **1999**, *201*, 93–102.
- Guallar, V.; Douhal, A.; Moreno, M.; Lluch, J. *J. Phys. Chem. A* **1999**, *103*, 6251–6256.
- Li, X.; Cai, Z.; Sevilla, M. *J. Phys. Chem. B* **2001**, *105*, 10115–10123.
- Kryachko, E.; Sabin, J. *Int. J. Quantum Chem.* **2003**, *91*, 695–710.
- Grebneva, H. *J. Mol. Struct.* **2003**, *645*, 133–143.
- Sobolewski, A.; Domcke, W. *Phys. Chem. Chem. Phys.* **2004**, *6*, 2763–2771.
- Herrera, B.; Toro-Labbe, A. *J. Chem. Phys.* **2004**, *121*, 7096–7102.
- Danilov, V.; Anisimov, V.; Kurita, N.; Hovorun, D. *Chem. Phys. Lett.* **2005**, *412*, 285–293.
- Shimizu, N.; Kawano, S.; Tachikawa, M. *J. Mol. Struct.* **2005**, *735*–736, 243–248.
- Villani, G. *Chem. Phys.* **2005**, *316*, 1–8.
- Villani, G. *Chem. Phys.* **2006**, *324*, 438–446.
- Liu, F.; Qian, P.; Yan, S.; Bu, Y. *J. Mol. Struct.: THEOCHEM* **2006**, *760*, 209–217.
- Perun, S.; Sobolewski, A.; Domcke, W. *J. Phys. Chem. A* **2006**, *110*, 9031–9038.
- Noguera, M.; Sodupe, M.; Bertrán, J. *Theor. Chem. Acc.* **2007**, *118*, 113–121.
- Noguera, M.; Bertrán, J.; Sodupe, M. *J. Phys. Chem. B* **2008**, *112*, 4817–4825.
- Rueda, M.; Kalko, S.; Luque, F.; Orozco, M. *J. Am. Chem. Soc.* **2003**, *125*, 8007–8014.
- Rueda, M.; Kalko, S.; Luque, F.; Orozco, M. *J. Am. Chem. Soc.* **2006**, *128*, 3608–3619.
- Gorb, L.; Podolyan, Y.; Dziekonski, P.; Sokalski, W.; Leszczynski, J. *J. Am. Chem. Soc.* **2004**, *126*, 10119–10129.
- Florián, J.; Leszczynski, J.; Scheiner, S. *Mol. Phys.* **1995**, *84*, 469–480.
- Zhanpeisov, N.; Leszczynski, J. *J. Phys. Chem. A* **1998**, *102*, 6167–6172.
- Zhanpeisov, N.; Leszczynski, J. *J. Mol. Struct. (THEOCHEM)* **1999**, *487*, 107–115.
- Gorb, L.; Leszczynski, J. *J. Am. Chem.* **1998**, *120*, 5024–5032.
- Alemán, C. *Chem. Phys.* **1999**, *224*, 151–162.
- Alemán, C. *Chem. Phys.* **2000**, *253*, 13–19.
- Shishkin, O.; Gorb, L.; Leszczynski, J. *J. Phys. Chem. B* **2000**, *104*, 5357–5361.
- Moroni, F.; Famulari, A.; Raimondi, M. *J. Phys. Chem. A* **2001**, *105*, 1169–1174.
- Sivanesan, D.; Sumathi, I.; Welsh, W. *Chem. Phys. Lett.* **2003**, *367*, 351–360.
- Podolyan, Y.; Gorb, L.; Leszczynski, J. *Int. J. Mol. Sci.* **2003**, *4*, 410–421.
- Lee, C.; Cho, M. *J. Chem. Phys.* **2006**, *125*, 114509.
- Herbert, H.; Halls, M.; Hratchian, H.; Raghavachari, K. *J. Phys. Chem. B* **2006**, *110*, 3336–3343.
- Kabelac, M.; Hobza, P. *Phys. Chem. Chem. Phys.* **2007**, *9*, 903–917.
- Park, H.; Nam, S.; Song, J.; Park, S.; Ryu, S. *J. Phys. Chem. A* **2008**, *112*, 9023–9030.
- Sukhanov, O.; Shishkin, O.; Gorb, L.; Leszczynski, J. *Struct. Chem.* **2008**, *19*, 171–180.
- Kumar, A.; Mishra, P.; Suhai, S. *J. Phys. Chem. A* **2005**, *109*, 3971–3979.
- Kumar, A.; Sevilla, M.; Suhai, S. *J. Phys. Chem. B* **2008**, *112*, 5189–5198.
- Hu, X.; Li, H.; Liang, W.; Han, S. *J. Phys. Chem. B* **2005**, *109*, 5935–5944.
- Shukla, M.; Leszczynski, J. *J. Phys. Chem. A* **2005**, *109*, 7775–7780.
- Kim, H.; Ahn, D.; Chung, S.; Kim, S.; Lee, S. *J. Phys. Chem. A* **2007**, *111*, 8007–8012.
- Michalkova, A.; Kosenkov, D.; Gorb, L.; Leszczynski, J. *J. Phys. Chem. B* **2008**, *112*, 8624–8633.
- Cerón-Carrasco, J. P.; Requena, A.; Michaux, C.; Perpète, E. A.; Jacquemin, D. *J. Phys. Chem. A* **2009**, *113*, 7892–7898.
- Gould, I.; Kollman, P. *J. Am. Chem. Soc.* **1994**, *116*, 2493–2499.
- Sponer, J.; Jurecka, P.; Hobza, P. *J. Am. Chem. Soc.* **2004**, *126*, 10142–10151.
- Jurecka, P.; Sponer, J.; Cerny, J.; Hobza, P. *Phys. Chem. Chem. Phys.* **2006**, *8*, 1985–1993.
- Cooper, W. *Biochem. Genet.* **1994**, *32*, 383–395.
- Becke, A. *J. Chem. Phys.* **1993**, *98*, 5648–5652.
- Perdew, J. *Phys. Rev. B* **1986**, *33*, 8822–8824.
- van der Wijst, T.; Guerra, C. F.; Swart, M.; Bickelhaupt, F. *Chem. Phys. Lett.* **2006**, *426*, 415–421.
- Boys, S.; Bernardi, F. *Mol. Phys.* **1970**, *19*, 553–566.
- Simon, S.; Duran, M.; Dannenberg, J. *J. Chem. Phys.* **1996**, *105*, 11024–11031.
- Michaux, C.; Wouters, J.; Jacquemin, D.; Perpète, E. A. *Chem. Phys. Lett.* **2007**, *445*, 57–61.
- Michaux, C.; Wouters, J.; Perpète, E. A.; Jacquemin, D. *J. Phys. Chem. B* **2008**, *112*, 2430–2438.
- Truhlar, D. *Chem. Phys. Lett.* **1998**, *294*, 45–48.
- Frisch, M. J.; Trucks, G. W.; Schlegel, H. B.; Scuseria, G. E.; Robb, M. A.; Cheeseman, J. R.; Montgomery, J. A., Jr.; Vreven, T.; Kudin, K. N.; Burant, J. C.; Millam, J. M.; Iyengar, S. S.; Tomasi, J.; Barone, V.; Mennucci, B.; Cossi, M.; Scalmani, G.; Rega, N.; Petersson, G. A.; Nakatsuji, H.; Hada, M.; Ehara, M.; Toyota, K.; Fukuda, R.; Hasegawa, J.; Ishida, M.; Nakajima, T.; Honda, Y.; Kitao, O.; Nakai, H.; Klene, M.; Li, X.; Knox, J. E.; Hratchian, H. P.; Cross, J. B.; Bakken, V.; Adamo, C.; Jaramillo, J.; Gomperts, R.; Stratmann, R. E.; Yazyev, O.; Austin, A. J.; Cammi, R.; Pomelli, C.; Ochterski, J. W.; Ayala, P. Y.; Morokuma, K.; Voth, G. A.; Salvador, P.; Dannenberg, J. J.; Zakrzewski, V. G.; Dapprich, S.; Daniels, A. D.; Strain, M. C.; Farkas, O.; Malick, D. K.; Rabuck, A. D.; Raghavachari, K.; Foresman, J. B.; Ortiz, J. V.; Cui, Q.; Baboul, A. G.; Clifford, S.; Cioslowski, J.; Stefanov, B. B.; Liu, G.; Liashenko, A.; Piskorz, P.; Komaromi, I.; Martin, R. L.; Fox,

D. J.; Keith, T.; Al-Laham, M. A.; Peng, C. Y.; Nanayakkara, A.; Challacombe, M.; Gill, P. M. W.; Johnson, B.; Chen, W.; Wong, M. W.; Gonzalez, C.; Pople, J. A. *Gaussian 03*, revision D.02; Gaussian, Inc.: Wallingford, CT, 2004.

(62) Flükiger, P.; Lüthi, H.; Portmann, S.; Weber, J. *Swiss Center for Scientific Computing*; Manno: Switzerland, 2000.

(63) Rosenberg, J.; Seeman, N.; Day, R.; Rich, A. *J. Mol. Biol.* **1976**, *104*, 145–167.

(64) Guerra, C. F.; Bickelhaupt, F.; Snijders, J.; Baerends, E. *J. Am. Chem. Soc.* **2000**, *122*, 4117–4128.

(65) Miura, S.; Tuckerman, M.; Klein, M. *J. Chem. Phys.* **1998**, *109*, 5290–5299.

(66) Topal, M.; Fresco, J. *Nature* **1976**, *263*, 285–289.

JP906551F